

Sensitivity Analysis of Tensioned–Leg Mooring Line Under Variations of Water Depth

Tengku Luqman Hakim Tengku Halim¹, Siow Chee-Loon^{1,2}, Arifah Ali¹, Lee Kee-Quen³ and Kang Hooi-Siang^{1,2,*}

¹Faculty of Mechanical Engineering
²Marine Technology Centre
Universiti Teknologi Malaysia
81310 UTM Johor Bahru
Johor, Malaysia

³Malaysia-Japan International Institute of Technology
Universiti Teknologi Malaysia
Jalan Sultan Yahya Petra
54100 Kuala Lumpur
Malaysia

ABSTRACT

Floating structures can provide an alternative solution to the developments in the highly populous urban area. The agile mobility and flexible of deployment for a floating solution are considered more effective in the nearshore areas where the conventional piling for construction of a fixed offshore structure is prohibited due to the protection of the diversity of marine lives. However, the sensitivity of its mooring system subjects to variations of water depth is of research interest. This paper discusses a numerical study of a cylindrical floating structure with its single mooring line connected to the seabed in a tensioned condition. The response of floater heave motion and in-line tension of mooring line for water depths of 300 m, 200 m, 100 m and 50 m were investigated. The mooring line is a steel wire rope subjects to the wave-induced motions of the floater. A numerical model of the floater was analyzed in hydrodynamic software, Ansys-Aqwa, under predefined environmental loading conditions to determine the in-line tension of the mooring system and the behaviors of the floater in a time domain. The results indicated that the floater oscillated at a vertical stiffness which magnitude is inversely proportional to the length of mooring lines. The ratio of the maximum in-line tension for mooring line in the 50 m water depth can be up to 1.52 to the original one in the 300 m water depth if the mooring line with an identical diameter is truncated. This study is significant to provide a reference for the mobility and redeployment of floating structures in locations with different water depth.

Keywords: Mooring line, tensioned-leg, water depth, floating structure

1.0 INTRODUCTION

A large floating structure has huge potential in the coastal areas of the island regions as an alternative hub to support the human's activities.

* Corresponding author : kanghs@utm.my

One of the major attractions to use floating solution is this is free from the competition of land acquisition, which could be a very cost-effective solution especially for the well-developed area where the rental price of land is relatively high. In the coastal regions, the water depth is relatively shallow. In the island regions of South East Asia, a majority of the coastal areas was surrounded by the water depth less than 100 m. A conventional type of fixed structure, such as jacket platform, is dominated in the coastline of this region. However, offshore piling for the construction of a fixed marine structure has been facing stricter regulations in the areas with a diversity of marine lives. The balance in between the environmental protection and the economic development calls for an advanced solution which has been identified as a floating solution.

The agile mobility of floating structure has enabled it to operate in multiple locations. For instance, a floating energy terminal is deployable in different locations according to seasonal energy consumptions. A floating fish farm, on the other hand, can be redeployed in another location if the water pollution at its original location is detected. The agile mobility of floating structure is highly depending on its station-keeping system where its mooring lines play a dominant role. Mooring line is a long cylindrical structure (LCS), which is regarded as a space curve [1, 2] in the deep-water oil and gas industry. The mooring line is excited by a highly complex motion which consisted of the forces and moments from wave [3, 4], current [5–7], platform motion [8] and self-excitation [9–11]. The interactions in between the floater and its mooring lines (and other LCS which connected the floater to the seabed) is one of the major research interests for the floating solution. The variations of water depth can cause the change of dynamic behaviors of the overall floater system. Yang and Xiao [12] investigated the dynamic instability of LCS subjects to the combined effects of parametric resonance and vortex excitation. They reported that parametric excitation is predominant to the instability in the severer sea states, whereas the vortex shedding contributes more to the instability when the sea state is milder. Coupled dynamics of the mooring lines and the floating platform motion can be simulated in a coupled time-domain dynamic-analysis program for floating bodies, mooring lines/tendons, and risers [2, 13–15]. Wang *et al.* (2015) studied the coupled dynamic of LCS under combined forcing and parametric excitation in deep water. Wang and Yang [8] investigated the behaviors of an LCS between two floating vessels under combined vortex excitations and they found that this combined effects can lead to huge displacement and damage of the LCS in deep water. Coupled equations which contain vortex-load and parametric excitation due to the floating platforms were developed in *Mathieu* equation. They concluded the combined excitations are larger than that subjected to only either vortex excitation or parametric instability [8].

This paper discusses the effects of water depth on the mooring line. The tensioned-leg mooring line is the focal subject of study. The main objectives of this paper are to (1) investigate numerically the heave motion of floater and (2) determine the in-line tension of tensioned-leg mooring line with respect to different water depths.

2.0 METHODOLOGY

2.1 Theoretical Modeling

A cylindrical floater is shown in Figure 1 where it is subjected to external excitation loads from waves. The floater is connected at its bottom to the seabed through a tensioned-leg mooring line. The in-line tension ΔT_{line} can be defined as:

$$\begin{aligned} \Delta T_{line} &= k_e \times \Delta L_{st} = \Delta B - W \\ &= k_e \times (h - d_d - z_B - L_{us}) = \Delta B - W \end{aligned} \quad (1)$$

where k_e is the equivalent stiffness of the mooring line, ΔL_{st} refers to the stretched length of the mooring line, ΔB is the changes of buoyancy force, and W is the weight of the floater. The geometry of mooring line stretched length ΔL_{st} is an output of water depth h , dynamic draught d_d , vertical coordinate of floater center of gravity z_B , and an unstretched length L_{us} of a mooring line. The equivalent stiffness of the mooring line is represented as:

$$k_e = \frac{E\pi D^2}{4\Delta L_{st}} \quad (2)$$

where E refers to the *Young* modulus of the material, and D is a diameter of the mooring line.

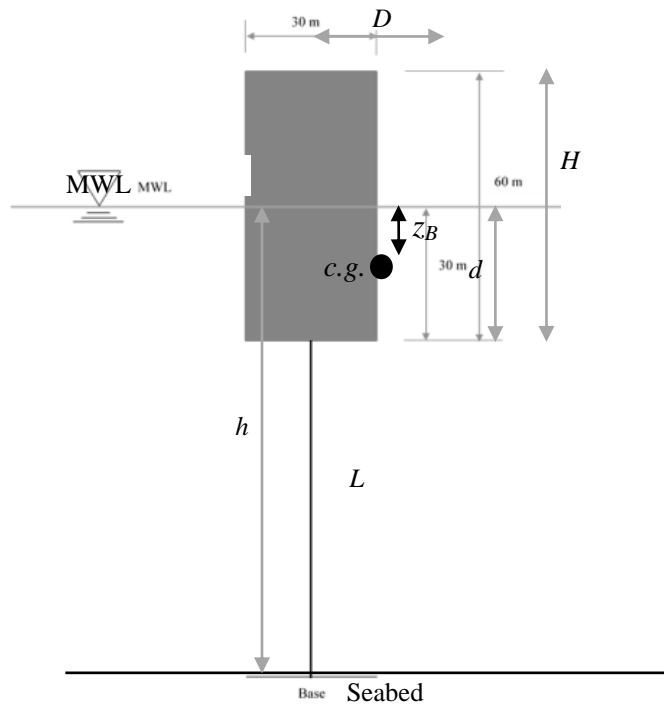


Figure 1: Floater at the initial condition

The net buoyancy to support the weight of floater and induced tension to the mooring line is defined as:

$$\Delta B - W = \rho_{sw} g \pi r^2 (d - z_B) \quad (3)$$

where ρ_{sw} refers to the density of seawater, g is the gravitational acceleration, r is the radius of the cylindrical floater and d is the draught of a floater.

2.2 Numerical Simulation

A model of cylindrical floater was modeled in AutoCAD software package and exported in the format of initial graphic exchange specification (IGES) to the *Ansys-*

Aqwa package for hydrodynamic analysis. The principal dimensions of the floater are shown in Table 1.

Table 1: Principal dimensions of floater

Height, H (m)	60
Outer diameter, D (m)	30
Draught at initial condition, d_0 (m)	30
Draught at free floating condition, d_f (m)	15
Initial vertical coordinate of c.g., z_B (m)	-15
Mass, m_f (kg)	1.082×10^7
Moment of inertia (I_{xx}, I_{yy}, I_{zz}) (kg.m ²)	$(3.85 \times 10^9, 3.85 \times 10^9, 1.22 \times 10^9)$
Moment of inertia (I_{xy}, I_{xz}, I_{yz}) (kg.m ²)	(0.0, 0.0, 0.0)
Density of sea water, ρ_{sw} (kg/m ³)	1025
Gravitational acceleration, g (m/s ²)	9.81

Note: c.g.: center of gravity of floater

The sensitivities of floater heave motion and in-line tension of tensioned-leg mooring line are investigated for a four different water depths h , which are 50 m, 100 m, 200 m and 300 m, respectively, as illustrated in Figure 2. The simulations are conducted under two parametrical cases as tabulated in Table 2. In Case A, the equivalent stiffness k_e is kept as a constant. Hence, the diameter of tensioned-leg mooring line will be reduced accordingly to the reduction of water depth. On the other hand, in Case B, the diameter of the mooring line is constant regardless of the water depth. The mooring line in Case B is an analogy of a truncated mooring line when the floater is relocated to shallower water regions.

In both cases, the floater subjects to wave excitation under regular wave train form. The wave direction comes from 0°. The wave height is 2 m and wave period is 10 s. The time series of wave input is shown in Figure 3.

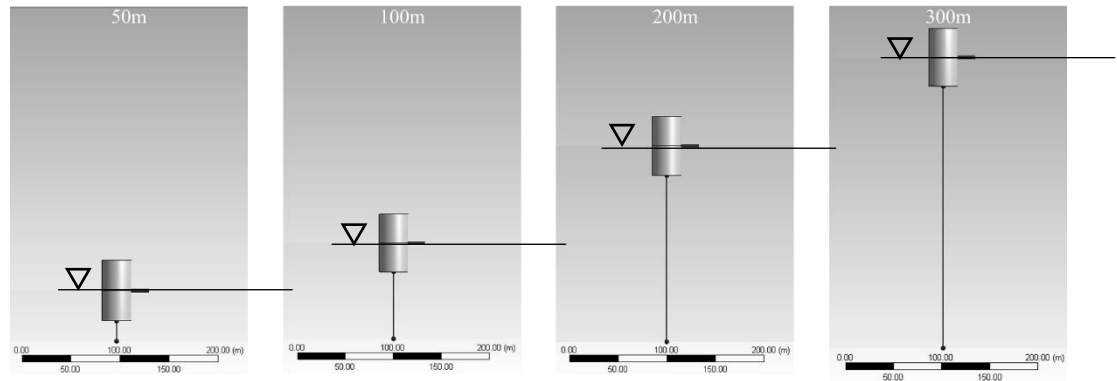


Figure 2: Setting of floater for water depth of (left to right): 50 m, 100 m, 200 m and 300 m

Table 2: Simulation cases for the sensitivity analyses

Water depth (m)	50	100	200	300
Case A: $k_e = \text{constant}, D_{\text{line}} = \text{variable}$				
Young modulus of line, E (GPa)	200	200	200	200
Diameter of line, D_{line} (m)	0.01	0.02	0.03	0.04
Equivalent stiffness, k_e (kN/m)	11070	11070	11070	11070
Unstretched length of line, L_{us} (m)	18.26	63.91	155.22	246.52
Case B: $k_e = \text{variable}, D_{\text{line}} = \text{constant}$				
Young modulus of line, E (GPa)	200	200	200	200
Diameter of line, D_{line} (m)	0.04	0.04	0.04	0.04
Equivalent stiffness, k_e (kN/m)	149445	42699	17582	11070
Unstretched length of line, L_{us} (m)	18.26	63.91	155.22	246.52

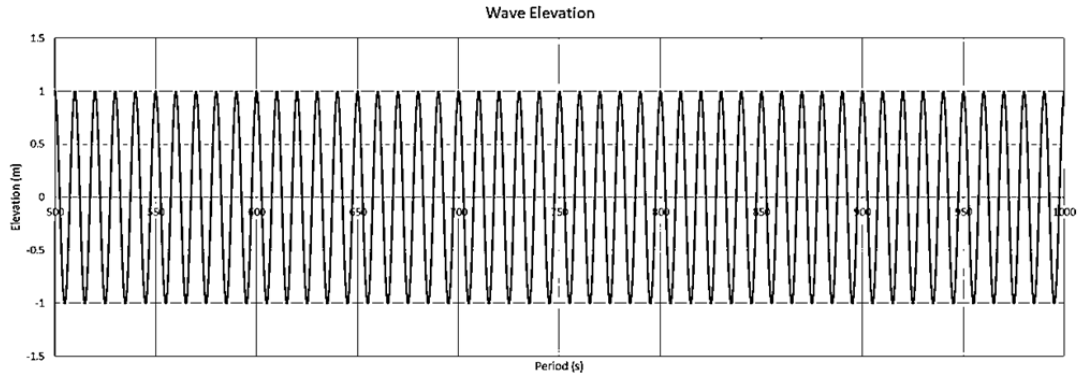


Figure 3: Wave input in regular form (wave amplitude = -1.0 m to 1.0 m, period = 10 s)

2.3 Grid Independent Test

The grid independent test of floater was conducted to identify the appropriate number of meshed elements for obtaining convergent results. Root mean square error (RMSE) for a different number of meshed elements was tested and the output is shown in Figure 4. In order to keep the RMSE below 10% of variations, a total element of 17002 was introduced to the simulations. The *Ansys-Aqwa* generated automatically the meshes by setting the defeaturing tolerance to 0.3 m and keeping the maximum size of a single element below 1.0 m.

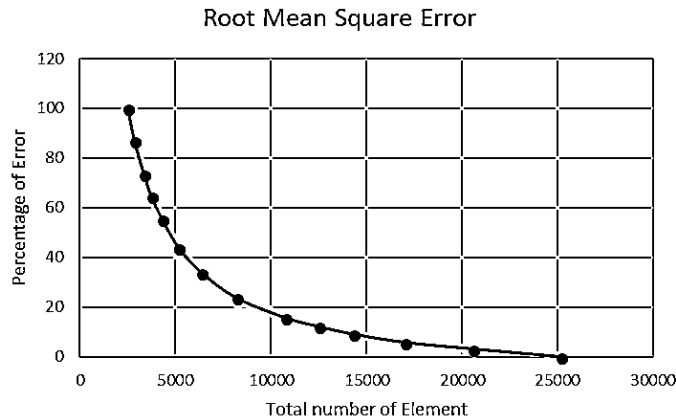


Figure 4: Percentage of RMSE with different number of meshed elements of floater

3.0 RESULTS AND DISCUSSION

The simulation results of the sensitivity tests for tensioned-leg mooring line under different water depths and both Cases A and B are tabulated in Table 3.

Table 3: Results of the numerical simulation

Water depth (m)	50	100	200	300
Case A: $k_e = \text{constant}$, $D_{line} = \text{variable}$				
Max. heave of <i>c.g.</i> (m)	5.02	2.36	-2.93	-8.07
Min. heave of <i>c.g.</i> (m)	4.59	2.00	-3.30	-8.78
Range of heave of <i>c.g.</i> (m)	0.43	0.36	0.37	0.71
Max. draught of floater, <i>d</i> (m)	25.41	28.00	33.30	38.78
Min. draught of floater, <i>d</i> (m)	24.98	27.64	32.93	38.07
Max. length of line, <i>L</i> (m)	25.02	72.36	167.07	261.93
Min. length of line, <i>L</i> (m)	24.59	72.00	166.70	261.22
Max. stretched length of line, L_{st} (m)	6.76	8.45	11.85	15.41

Min. stretched length of line, L_{st} (m)	6.33	8.09	11.48	14.70
Max. in-line tension, T_{line} (kN)	76369	93582	131222	170698
Min. in-line tension, T_{line} (kN)	70034	86542	127006	162758
Range of tension (kN)	6335	7040	4216	7940
Case B: k_e = variable, D_{line} = constant				
Max heave of $c.g.$ (m)	-0.97	-2.79	-5.96	-8.07
Min. heave of $c.g.$ (m)	-0.99	-3.39	-6.47	-8.78
Range of heave of $c.g.$ (m)	0.02	0.60	0.51	0.71
Max. draught of floater, d (m)	30.99	33.39	36.47	38.78
Min. draught of floater, d (m)	30.97	32.79	35.96	38.07
Max. length of line, L (m)	19.03	67.21	164.04	261.93
Min. length of line, L (m)	19.01	66.61	163.63	261.22
Max. stretched length of line, L_{st} (m)	0.77	3.30	8.82	15.41
Min. stretched length of line, L_{st} (m)	0.75	2.70	8.31	14.70
Max. in-line tension, T_{line} (kN)	115750	140832	155130	170698
Min. in-line tension, T_{line} (kN)	112365	115853	146212	162758
Range of tension (kN)	3385	24978	8918	7940

3.1 Case A: Constant Equivalent Stiffness of Mooring Line

In Case A, the equivalent stiffness of mooring line was in constant. The heave motion of the $c.g.$ for the floater under variations of water depth is shown in Figure 5. The heave motion of floater was captured from the simulation time series from the 500th second to the 1000th second where the system was assumed to be in a steady-state. Since the excitation wave load is in regular form, the heave motion of the floater is in generally regular for all the water depths. It is noteworthy that the position on the vertical axis refers to the coordinates at the vertical direction in the global axes system. The ratio for the range of heave motion of the $c.g.$ to the corresponding water depth are 0.86%, 0.36%, 0.19%, and 0.24% for water depths 50 m, 100 m, 200 m, and 300 m, respectively.

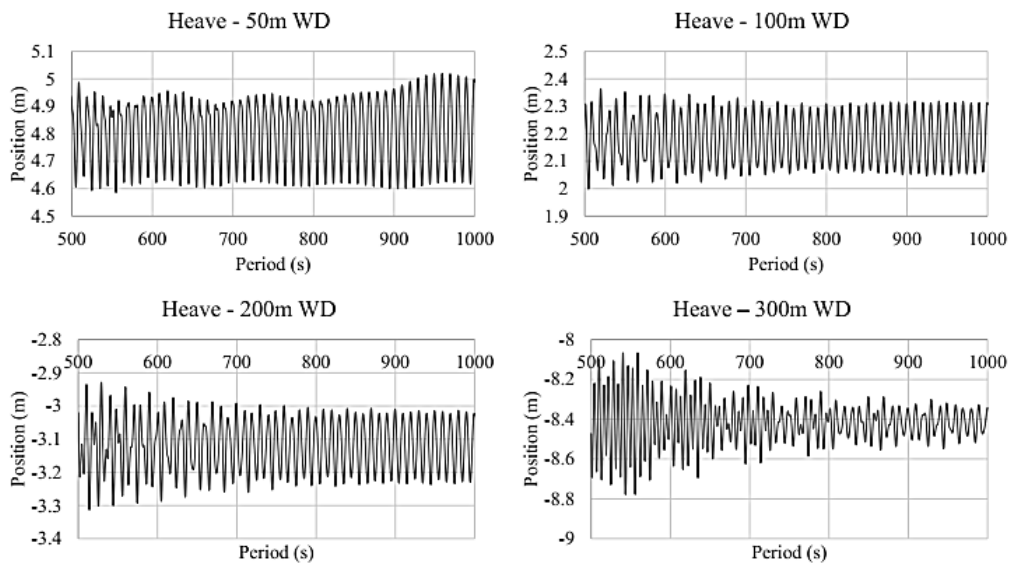


Figure 5: Heave of the $c.g.$ for floater under different water depths in Case A, where the position refers to the coordinates at the vertical direction in global axes system

Similarly, the in-line tension of mooring line under different water depths for Case A is shown in Figure 6. The maximum in-line tension of mooring line is 76369 kN, 93582 kN, 131222 kN and 170698 kN for water depths, 50 m, 100 m, 200 m and 300 m, respectively. The shallower water depth, the smaller in-line tension ΔT_{line} was obtained because the stretched length ΔL_{st} of mooring line is shorter accordingly. The maximum strains of the line elongation L_{st}/L_{us} during the steady-state are 37.0%,

13.2%, 7.6% and 6.3% for water depths 50 m, 100 m, 200 m and 300 m, respectively. From the phase portrait in Figure 8, it can be concluded that the simulation system is in dynamical stable condition for all these four water depths, where the loci of the plots are all in convergence.

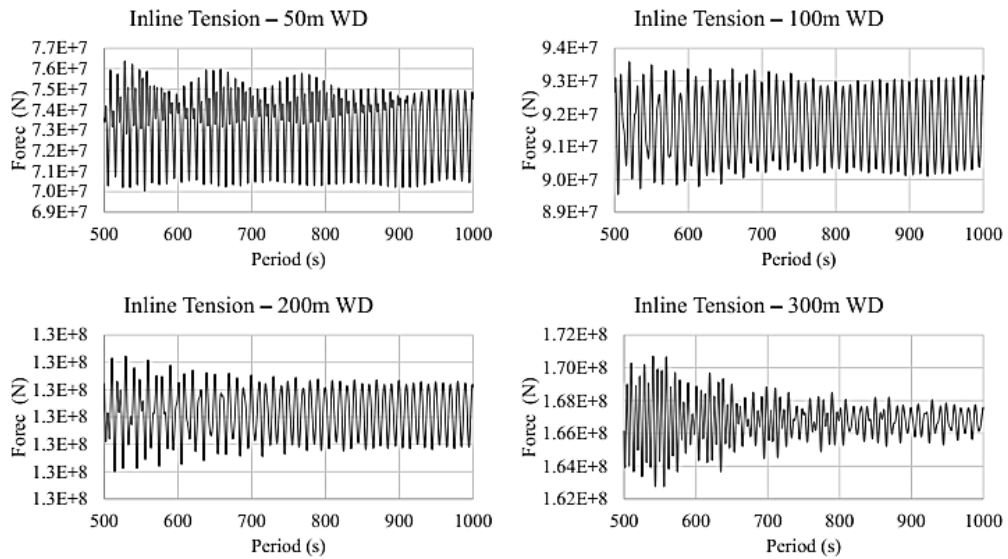


Figure 6: In-line tension of mooring line under different water depths in Case A

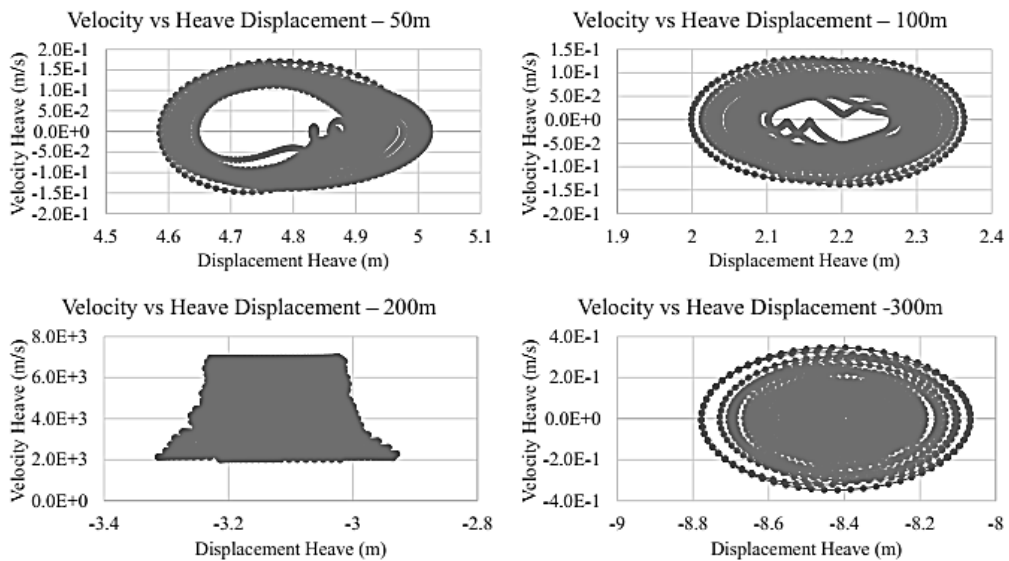


Figure 7: Phase portrait of the floater in heave direction for different water depths in Case A

3.2 Case B: Constant Diameter of Mooring Line

In Case B, the diameter of the mooring line was in constant. The equivalent stiffness k_e is changing inverse proportionally to the stretched length of mooring line ΔL_{st} as followed the Equation (2). The heave motion of the *c.g.* for the floater under variations of water depth is shown in Figure 8. Again, the heave motion of floater was captured from the simulation time series when the system was assumed in a steady-state. Since the equivalent stiffness in water depth 50 m is 13.5 times larger than the one in the water depth 300 m, the mooring line will become stiffen when the original mooring line of a floater in deeper water is directly redeployed and truncated in a shallower water region. Hence, it can be found that the floater in Case B has deeper draught in generally than the one in the Case A because a smaller elongation ΔL_{st} of

thicker mooring line (larger $\pi D^2/4$) can provide comparably sufficient restoring force to keep the position of the floater, as suggested in Equation (1). It can be verified by the maximum strains of the line elongation L_{st}/L_{us} during the steady-state in Case B are only 4.2%, 5.2%, 5.7% and 6.3% for water depths 50 m, 100 m, 200 m and 300 m, respectively.

The in-line tension of mooring line under different water depths for Case B is shown in Figure 9. The ratio of maximum inline tension for mooring line in Case B compared to Case A are 1.52, 1.50, 1.18 and 1.00 for water depths 50 m, 100 m, 200 m and 300 m, respectively. Therefore, a larger in-line tension is expected if the diameter of the mooring line is maintained and the length is truncated from a deeper to a shallower water. From the phase portrait in Figure 10, it can be concluded that the simulation system is in dynamical stable condition for all these four water depths in Case B, where the loci of the plots are all in convergence.

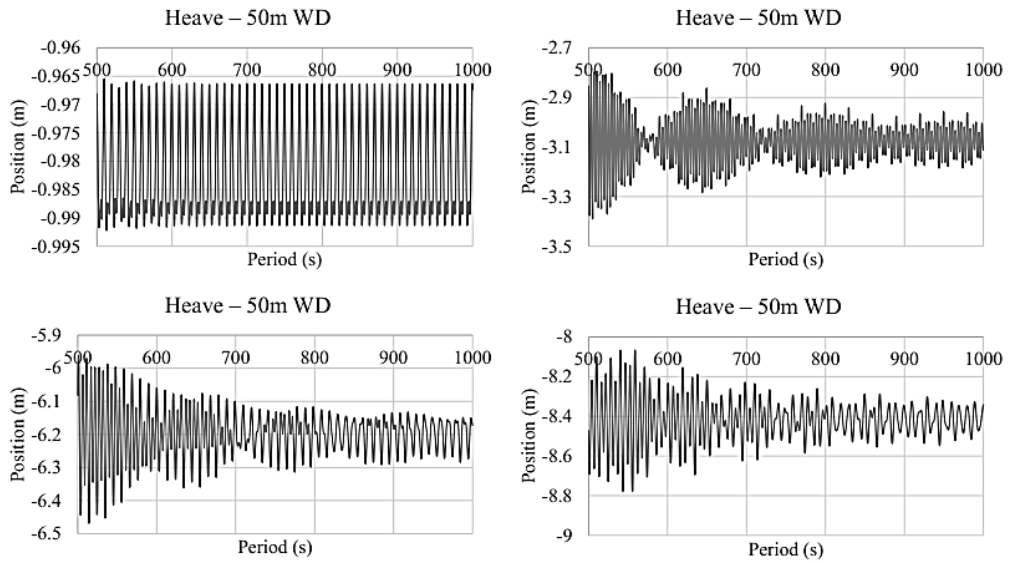


Figure 8: Heave of the *c.g.* for floater under different water depths in Case B, where the position refers to the coordinates at the vertical direction in global axes system

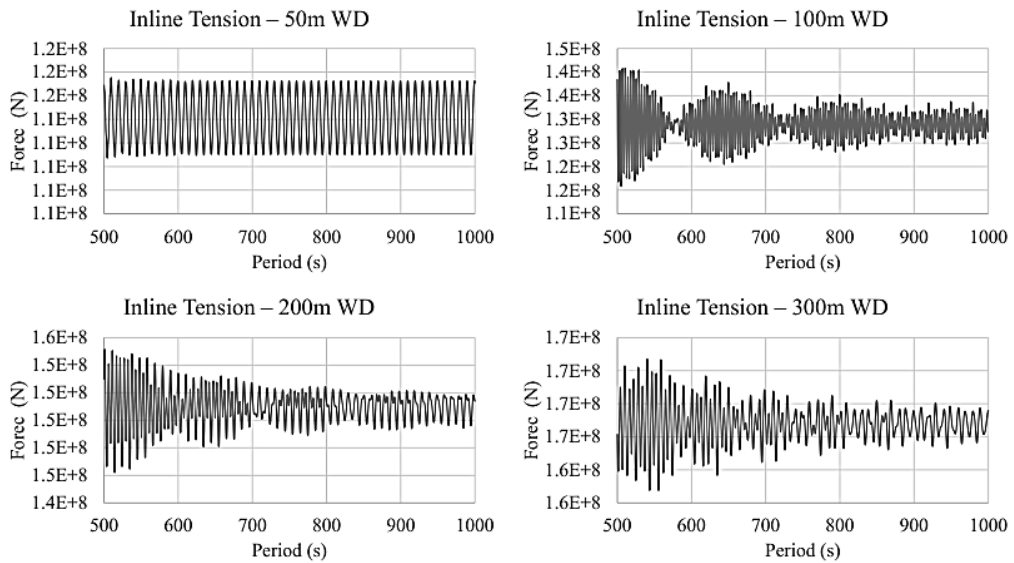


Figure 9: In-line tension of mooring line for different water depths in Case B

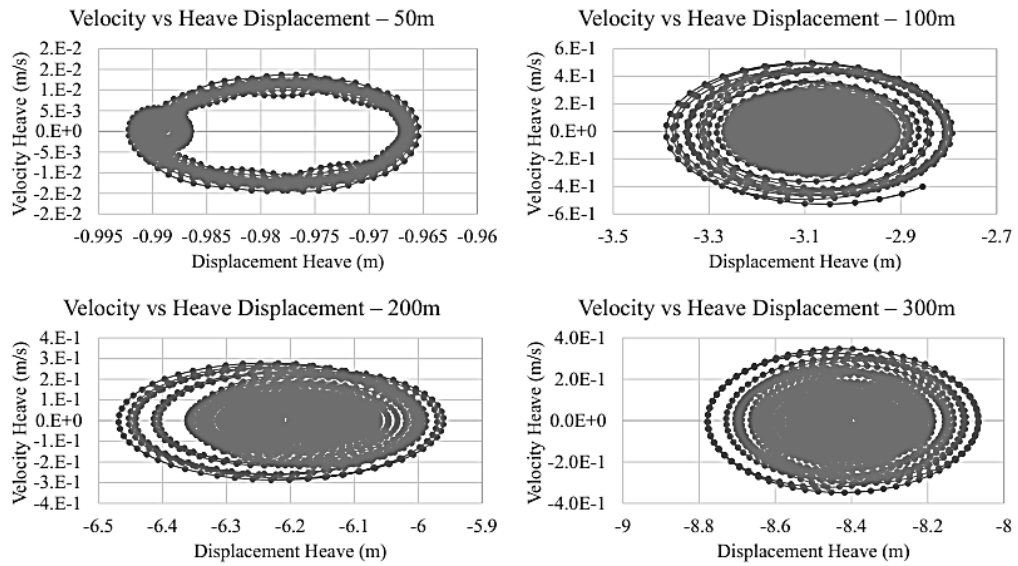


Figure 10: Phase portrait of the floater in heave direction for different water depths in Case B

3.3 Compensation of In-line Tension

In this analysis, we simulate how much difference of the in-line tension of mooring line if a floater was relocated from its original position with a water depth of 300 m to other locations (which have a water depth of 200 m, 100 m and 50 m, respectively). The differences between both Cases A and B are compared. It can be found that when the equivalent stiffness is maintained as in Case A, a larger difference of in-line tension is generated as compared to Case B, where the length of mooring line is truncated but the diameter of original mooring is intact. Hence, to change the mooring line diameter can provide a more sensitive in-line tension control in the new locations. However, in term of practicality, this option may be not cost-effective because the floater needs to be attached to a different mooring line in order to keep original vertical restoring force.

4.0 CONCLUSION

The sensitivity of water depth on a tensioned-leg mooring was presented. The main findings can be concluded as:

- If the equivalent stiffness of mooring line is constant when the floater is relocated, a mooring line with different diameter is needed to replace the original one. The heave motion of the *c.g.* for the floater is in generally regular for all the water depths as the wave input is in regular form. The shallower the water depth, the smaller in-line tension was obtained as the stretched length of the mooring line is accordingly shorter. The maximum strain of the line elongation L_{st}/L_{us} during the steady-state is 37.0% for a water depth of 50 m.
- When the diameter of mooring line is constant and the length is truncated, the equivalent stiffness in water depth 50 m is 13.5 times larger than the one in the water depth 300 m, hence the mooring line becomes more stiff when the original mooring line of a floater in deeper water is directly redeployed and truncated in a shallower water region. A larger in-line tension is expected in this case.

ACKNOWLEDGMENTS

The authors would like to thank the Universiti Teknologi Malaysia for supporting the research and providing the GUP grant (Vote No.: 03G92).

REFERENCES

1. Garrett D.L., 1982. Dynamic Analysis of Slender Rods, *J. Energy Resour. Technol.*, 104(4): 302–306.
2. Ran Z., 2000. *Coupled Dynamic Analysis of Floating Structures in Waves and Currents*, Doctoral Dissertation, Texas A&M University.
3. Xiao F. and Yang H.Z., 2014. Probabilistic Assessment of Parametric Instability of A Top Tensioned Riser in Irregular Waves, *J. Mar. Sci. Technol.*, 19(3): 245–256.
4. Radhakrishnan S., Datla R. and Hires, R.I., 2007. Theoretical and Experimental Analysis of Tethered Buoy Instability in Gravity Waves, *Ocean Eng.*, 34(2): 261–274.
5. Kang H.-S., Tang C.H.-H., Quen L.K., Steven A. and Yu X., 2016. Prediction on Parametric Resonance of Offshore Crane Cable for Lowering Subsea Structures, *2016 IEEE International Conference on Underwater System Technology: Theory and Applications (USYS)*, IEEE, Penang, Malaysia, 165–170.
6. Lucor D. and Triantafyllou M.S., 2008. Parametric Study of A Two Degree-of-Freedom Cylinder Subject to Vortex-Induced Vibrations, *J. Fluids Struct.*, 24(8): 1284–1293.
7. Lee K.Q., Abu A., Muhamad P., Tan L.K., Kang H.S., Tang H.H. and Toh H.T., 2017. Prediction on the Performance of Helical Strakes Through Fluid-Structure Interaction Simulation, *Communications in Computer and Information Science*, Springer Verlag, Singapore, 538–547.
8. Wang Z. and Yang H., 2016. Parametric Instability of A Submerged Floating Pipeline between Two Floating Structures Under Combined Vortex Excitations, *Appl. Ocean Res.*, 59: 265–273.
9. Yang H., Xiao F. and Xu P., 2013. Parametric Instability Prediction in A Top-Tensioned Riser in Irregular Waves, *Ocean Eng.*, 70: 39–50.
10. Kang H.-S., Wu Y.-T., Quen L.K., Tang C.H.-H. and Siow C.-L., 2017. Underwater Target Tracking of Offshore Crane System in Subsea Operations, *Communications in Computer and Information Science*, Springer Verlag, Singapore, 126–137.
11. Akcabay D.T. and Young Y.L., 2015. Parametric Excitations and Lock-in of Flexible Hydrofoils in Two-Phase Flows, *J. Fluids Struct.*, 57: 344–356.
12. Yang H. and Xiao F., 2014. Instability Analyses of a Top-Tensioned Riser Under Combined Vortex and Multi-Frequency Parametric Excitations, *Ocean Eng.*, 81: 12–28.
13. Kim M.H. and Koo W.C., 2005. 2D Fully Nonlinear Numerical Wave Tanks, *Numerical Models in Fluid-Structure Interaction*, WIT Press, 43–81.
14. Bae Y.H. and Kim M.-H., 2013. Influence of Failed Blade-Pitch-Control System to FOWT by Aero-Elastic-Control-Floater-Mooring Coupled Dynamic Analysis, *Ocean Syst. Eng.*, 3(4): 295–307.
15. Kang H.-S., Kim M.-H., Bhat Aramanadka S.S. and Kang H.-Y., 2014. Dynamic Response Control of Top-Tension Risers by A Variable Damping and Stiffness System with Magneto-Rheological Damper, *ASME 2014 33rd International Conference on Ocean, Offshore and Arctic Engineering (OMAE)*, Volume 6A: Pipeline and Riser Technology, San Francisco, California, USA.